Icing Wind Tunnel Tests on the CSIRO Liquid Water Probe†

W. D. KING,* J. E. DYE,** J. W. STRAPP,@ D. BAUMGARDNER,** AND D. HUFFMAN***

*Visitor to the National Center for Atmospheric Research from CSIRO Cloud Physics Laboratory, Sydney, Australia
**National Center for Atmospheric Research, Boulder, CO 80307+
@Atmospheric Environment Service, Downsview, Ontario, Canada M3H 5T4
***Particle Measuring Systems, Inc., Boulder, CO 80301

(Manuscript received 12 July 1984, in final form 11 February 1985)

ABSTRACT

Wet wind tunnel tests have been performed on several versions of the CSIRO probe designed for the airborne measurement of liquid water content. Four different controller units and 17 different probe sensors (including half-size and shielded versions) were tested. Even with tests conducted under extreme conditions, differences in response for all units were always less than 15%, except for the shielded units which needed to be operated at least 60°C hotter than the unshielded ones to yield the same output. Probe measurements with the unshielded sensors were typically within 5% and always within 10% of the tunnel values which were determined from icing cylinder measurements. The short length probes performed equally as well as the standard length ones and have certain operational advantages, such as greater robustness and the ability to operate at higher liquid water contents for a given supply voltage. Changing airspeed from 15 to 100 m s^{-1} and ambient temperature from −28°C to +10°C produced no measurable effect on any probe response, whereas grossly overdamping the probes via incorrect offset voltages could reduce the apparent output sensitivity by as much as 50%.

1. Introduction

Many research organizations are now using the CSIRO probe for airborne measurements of liquid water content (LWC). Currently at least 15 groups are using either their own version of the original design described in King *et al.* (1978) or the commercial version marketed by Particle Measuring Systems (PMS) of Boulder, Colorado. Although the probe has been subjected to a variety of comparisons, (Baumgardner, 1983) thermal and electronic tests (King *et al.*, 1978; Bradley and King, 1979; King *et al.*, 1981) it was felt that a series of icing wind tunnel comparisons and calibrations of the type performed on the Johnson–Williams (JW) probe by Strapp and Schemenauer (1982) would help to evaluate the performance of the probe. This paper describes a series of such tests.

There were four major objectives of these tests: (i) to determine the differences, if any, between the PMS version of the probe and the version currently used by CSIRO; (ii) to determine the reliability of the calibration of both versions; (iii) to check the performance of both under typical aircraft operating conditions; and (iv) to test several short probe elements that were designed to improve robustness and have the ability to measure higher liquid water contents.

† Neither the National Center for Atmospheric Research nor the Atmospheric Environment Service approves, recommends or endorses any proprietary product mentioned in this publication. No reference shall be made to NCAR or AES or this publication in any advertising or sales promotion which would indicate or imply that NCAR or AES approves or does not approve, recommends, or endorses any proprietary product mentioned herein.

+ The National Center for Atmospheric Research is sponsored by the National Science Foundation.

2. Tunnel properties

The icing tunnel operated by the Low Temperature Laboratory of the Mechanical Engineering Division of the National Research Council (NRC) of Canada was used for these tests. A good description of the tunnel can be found in Strapp and Schemenauer (1982), and Lozowski *et al.* (1983). In brief, the tunnel has a working cross section of 30 cm × 30 cm, and can produce a LWC of up to 4 g m^{-3} at 50 m s^{-1}, with proportionately less LWC as the speed is increased up to a maximum of approximately 150 m s^{-1}. The operating temperature range extends from room temperature down to −40°C, and the tunnel can be operated at subatmospheric pressures, although this feature was never utilized. In the runs described in this paper, the tunnel was operated from −28 to +10°C, at speeds from 15 to 100 m s^{-1}. Two probes were tested during each run. This not only reduced the number of required runs, but also allowed for tunnel irregularities to be distinguished from instrument output irregularities.

a. Tunnel calibration

The tunnel calibration is performed by taking icing cylinder measurements whereby the LWC is computed from the mass of ice accreted on a cylinder of known dimensions during a given time interval. Based on the work of Stallabrass (1978), this method of calibration is thought to be accurate in an absolute sense to better than 10%. The icing cylinder technique provides an excellent comparison with the hot-wire probe for two reasons:

(i) Since the cylinder and hot wires have similar diameters, the calculated LWC is insensitive to the assumed droplet diameter. In these tests, a single droplet size distribution, with median volume diameter of 20 μm and cutoff at about 30 μm, was used for all tests based on previous investigations of the output from the nozzles. For this size distribution, the maximum allowance for collection efficiency at the lowest operating speed of 15 m s^{-1} was 6%. Had the mean volume diameter been as low as 10 μm or as high as 30 μm [recent work with a Forward Scattering Spectrometer Probe (FSSP) has suggested that under some circumstances it could possibly be as low as 16 μm], absolute errors of less than 13% would have been produced. In a comparative sense, the situation is more favorable than this because the diameter of the icing cylinder (2.48 to typically 4.2 mm) and the CSIRO probes (1.8 to 2.2 mm) were sufficiently close for the maximum differences in collection efficiencies to be less than 3%. Collision efficiencies were all calculated according to an NRC refinement of the Langmuir and Blodgett (1961) technique (see Stallabrass, 1978), with the icing cylinder collections based on the mean diameter of the cylinder during accretion.

(ii) Both the mass accreted by the icing cylinder and the power consumed by the hot-wire probe are proportional to the liquid water flux, i.e., the product of the LWC and the air velocity. Thus, for comparison purposes, the need for accurate separate monitoring of the air velocity is eliminated. If the rate at which water is emitted from the nozzles remains constant, then fluctuations in the air velocity are unimportant as long as they are not large enough to change such parameters as the distribution of water across the tunnel, droplet collection efficiencies, or the dry air power loss from the wire. During the runs at subzero temperatures, it was usual for the tunnel velocity to decrease by as much as 3% due to rime buildup in the tunnel, but never by more than 5%.

The icing cylinder technique is comparatively insensitive to the density of the ice accreted on the cylinder. For typical masses accreted during a run, changing the assumed ice density from 0.7×10^3 to 0.92×10^3 results in changes in the calculated LWC of 6%. An ice density of 0.88 kg m^{-3} was used in all the icing cylinder measurements described in this paper, a value based on the measurements of Stallabrass (1978).

Tunnel calibration curves of LWC against total water flow rate for 50, 75, and 100 m s^{-1} are shown in Fig. 1. Apart from the circled points for 75 m s^{-1}, the curves are smooth and very close to those obtained six months earlier, also shown. The circled points are low as the result of a tunnel limitation at high liquid water contents. Between the nozzles and the flow meters measuring the water flow, there is a pressure activated valve which is used to divert the water flow to a drain. This valve allows the operator to set up the desired water flow without turning on the nozzles, thereby reducing the time that water is sprayed into the tunnel, an important consideration in terms of ice build-up on the tunnel. During the latter third of the tests, it was found that at the highest water flow rate, when the air pressure to the nozzles was also at its maximum, the drain valve sometimes was forced partially open, shunting water from the nozzles to the drain. Since the water flow rate measured at the meters remained constant, the operator had no means of knowing that the LWC in the tunnel was less than it should be. Thus the circled points have been ignored in the tunnel calibration curves, as have any other data points obtained at maximum nozzle air pressure. It is not known if this problem influenced previous work done in this tunnel at high LWCs, although some of the curves in Strapp and Schemenauer (1982) exhibit a similar behavior.

When the tunnel LWCs are plotted against nozzle flow rate per unit air velocity (Fig. 2), there are small differences between the 50, 75, and 100 m s^{-1} curves. These small velocity-dependent effects could be a reflection of incorrect allowance for collection efficiencies, differing distributions of water across the tunnel at different speeds, etc. In any case, they are sufficiently small to demonstrate that the air velocity does not need to be monitored accurately for each separate test.

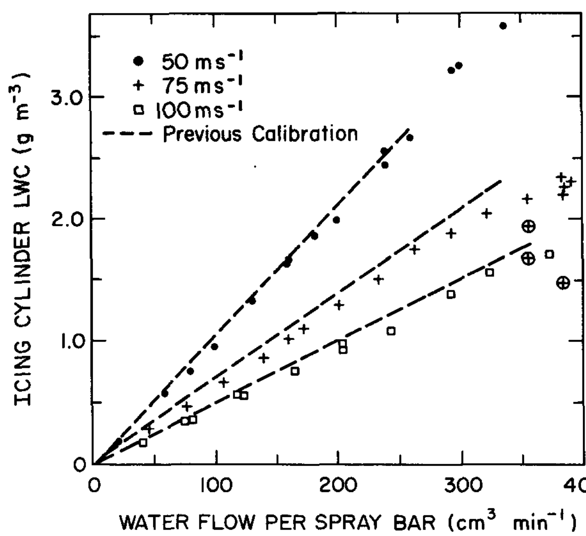

FIG. 1. Liquid water content determined from rotating icing cylinders as a function of flow rate through the spray bars for the NRC icing wind tunnel. The circled plus signs denote questionable points (see text).

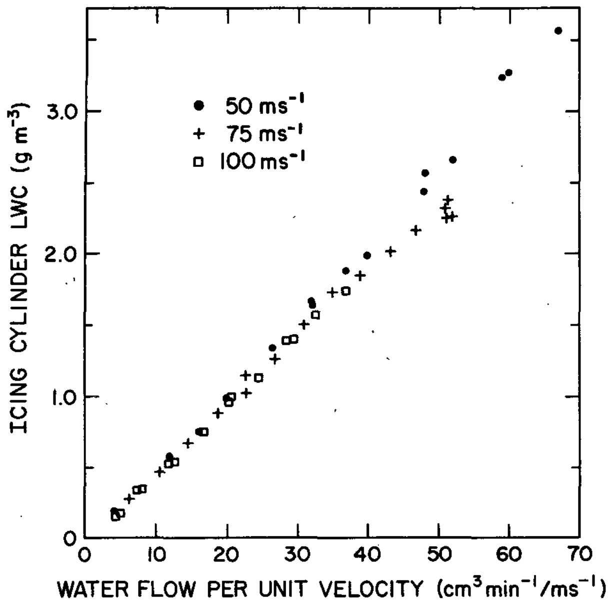

FIG. 2. Liquid water content determined from icing cylinder measurements plotted as a function of water flow rate normalized to the wind tunnel airspeed.

b. Tunnel profiles

Vertical and horizontal profiles of air velocity and LWC were taken at a variety of positions. The results normalized to the values at the center of the tunnel are shown in Fig. 3. (Use of the CSIRO probe to produce the water profiles presupposes that the probe response is linear in the range of LWC and airspeed investigated. Evidence to support this assumption will be given later.) The velocity profile is extremely flat, with maximum velocity differences of 1.5% occurring near the tunnel walls.

The LWC profiles are not as flat, with differences of up to 50% near the tunnel walls. At the probe positions, also shown in Fig. 3, differences from the center value of about 5% are more typical. Since the icing cylinder collections were always carried out in the middle of the tunnel, all of the probe results were increased by 4.5% to allow for their offset in the vertical. No allowance was made for offset in the horizontal direction because the lengths of the icing cylinder and the master elements of the probes are quite similar.

3. Probes used

In all, four different control boxes and 17 different probe elements were used. Of the four control boxes, three were made by PMS, and modified as described later, and the remaining one made to CSIRO specifications. The controller circuits in both PMS and CSIRO versions use different components, but are identical in terms of operating principle except for the insertion of the offset voltage required for damping purposes. This difference is discussed in Section 6h. A schematic of the controller circuitry is given in Fig. 4.

Previous tests in the NRC tunnel on the PMS probes had produced results that pointed to the need for changes in some aspects of the probes' construction. Accordingly, before using the standard PMS control boxes, the following modifications were made:

i) The input to amplifier A_2 was taken from pins on the connector on the probe base instead of inside the control box, by running two extra leads from the probe to the controller. Without these extra leads, A_2 senses the voltage drop across the master element plus the drop along the lead wires from the control box to the probe. This can cause overestimates of LWC by 3 to 5%.

ii) The gain of amplifier A_2 was reduced from ⅔ to ½. With a gain of ⅔ and a standard length element, amplifier output would limit at an LWC of about 2.5 g m^{-3} at 75 m s^{-1}.

iii) The output voltage for recording purposes was taken from the output of amplifier A_5 at the control box rather than at a later stage in the display box. This step was taken because the PMS wiring contained no provision for a separate analog signal return line, and sharing the signal return with the power return underestimates the LWC by the order of 5% at low LWCs.

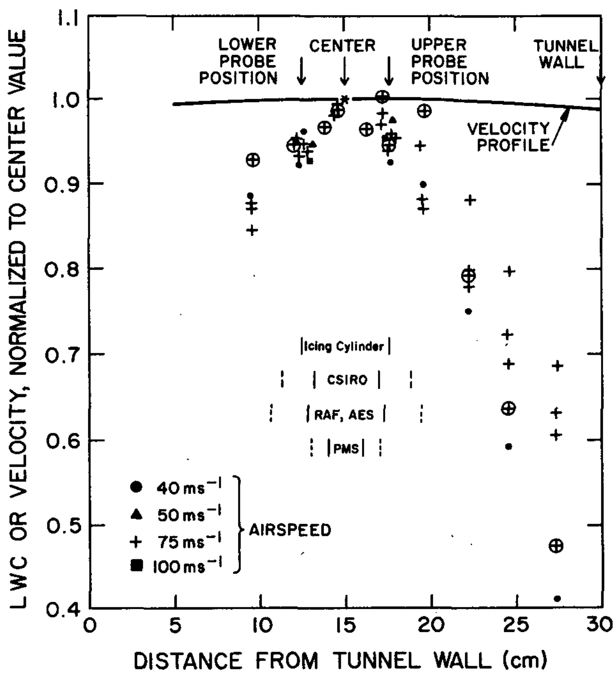

FIG. 3. Horizontal and vertical profiles of velocity and liquid water content across the tunnel normalized to the value in the center. Different airspeeds are denoted by symbols shown in the legend and values for horizontal profile runs are circled. The comparative dimensions of the icing cylinder, and the lengths of master (solid lines) and slave (dashed lines) for different sensors are also shown.

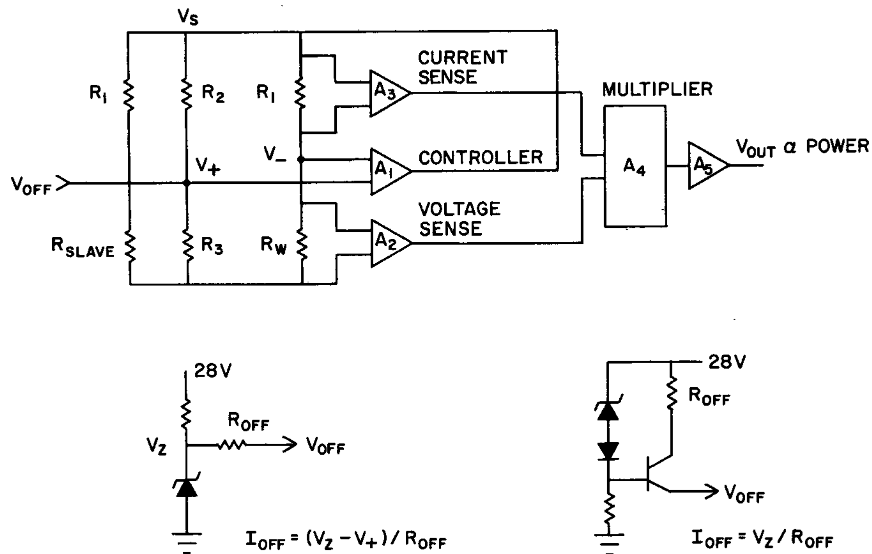

FIG. 4. A simplified schematic of the control circuitry of the CSIRO probe with the methods of introducing offset current used by PMS (lower left) and CSIRO (lower right) shown.

The 17 probe elements belonged to five different subgroups: standard PMS, standard CSIRO, Convective Storms Division PMS/(CSD) short (standard diameter), PMS/CSD short (larger diameter) and PMS/CSD short (shielded). The dimensions are given in Table 1 with a photograph in Fig. 5. The shorter probes were designed by CSD of NCAR and PMS with two major advantages in mind: (i) To increase the maximum LWC that can be measured. (The longer sensors were expected to be limited by the 28 V supply at around 3 g m^{-3} at 75 m s^{-1}.) (ii) To increase the robustness of the sensor, because some users had reported breakage problems. The shielded version (i.e., another nickel–silver tube of wall thickness 0.1 mm is placed in a very tight fit over the outside of a normal probe) was intended to be even more rugged. In total, the array of probe elements allowed testing of sensors with a spread of 2.1:1 in length, and 1.5:1 in diameter.

The PMS probes were equipped with 60 W de-icing heaters on each probe tip whilst the CSIRO-built units had no form of de-icing.

4. Analysis of probe data

The analog voltage for each probe was monitored using a digital voltmeter, a digital data acquisition system recording at 1 Hz, and recorded on a chart recorder usually operated at 1 mm s^{-1} but occasionally at chart speeds up to 125 mm s^{-1} to examine the high speed response. A typical chart record for a series of measurements at 75 m s^{-1} and 10°C is shown in Fig. 6. When the tunnel water was first turned on, some slight flow meter adjustments were necessary (Fig. 6). The LWC was calculated from the difference in average probe power before the water was turned on and after the flow meter adjustments were made. Averaging periods were typically 15 to 30 s. If this difference in power, the wet power, is denoted by P_w, then

$$P_w = [L(T_e) + c(T_e - T_a)]ldwvE(d)f, \quad (1)$$

where $L(T_e)$ is the latent heat of vaporization of water at the evaporation temperature T_e, c the specific heat of water, T_a the air temperature, l and d the probe length and diameter respectively, w the LWC, v the air velocity, $E(d)$ the collection efficiency, and f the tunnel

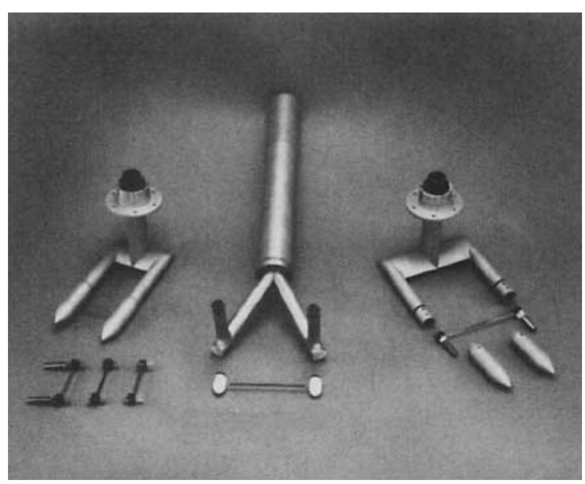

FIG. 5. Photographs of various versions of the probe and sensors: (left) PMS/CSD short probe with various sensors in front; (middle) CSIRO-made probe and sensor; (right) standard PMS probe showing sensor with heaters and heater caps disassembled.

TABLE 1. Characteristics of probe sensors used.

Name	Type	Manufacture	Master l (mm)	Master d (mm)	Overall length (mm)
CSIRO	Standard construction	CSIRO	38	1.76	83
RAF	Standard construction	PMS	42.5	1.90	90
AES	Standard construction	PMS	42.5	1.90	90
PMS-USA	Standard construction, short	PMS/CSD	19.95	1.76	47.5
PMS-USB	Large diameter, short	PMS/CSD	19.95	2.25	47.5
PMS-SA	Shielded, short	PMS/CSD	19.95	2.01	47.5

position factor as described in Section 2b. The probe diameter was measured to an accuracy of 0.01 mm, the length to 0.02 mm, T_e taken as 80°C (causing a maximum error of 1.5%—see King *et al.*, 1981), P_w could be measured to an accuracy of about 3%, f is considered accurate to 1%, and the comparative error in calculating $E(d)$ from the NRC modified Langmuir and Blodgett data is much less than 3%. The net result is that for the tests, the LWC could be calculated with a comparative accuracy (i.e., relative to the wind tunnel icing cylinder values) of about 8%.

In these tests, no attempt was made to investigate the relationship describing the power dissipated by the probe under dry conditions. It is considered that the relationship and analysis techniques given in King *et al.* (1981) are sufficiently accurate (typically 1 to 2%) for most users of the probe. In brief, we recommend a nonlinear regression to estimate the wire temperature and heat transfer coefficients simultaneously. Stability of the electronic components is a prerequisite for accurate reproducibility of the dry power (see Section 2b of King *et al.*, 1981).

5. Comparisons

a. All probes, 75 m s^{-1}, 10°C

The data from all probes operated with correct wire temperature and offset voltage for 75 m s^{-1} and +10°C are shown in Fig. 7. (In tests described later, some of the set-up parameters were taken to extreme values to observe the effect, and these results are not included in Fig. 7.) The agreement between all the probes under these conditions is remarkably good, with the standard deviation at 1.9 g m^{-3} being less than 0.15 g m^{-3}. The best-fit linear regression line through all the points has a slope of 0.978 so that on average, the probes are yielding liquid water contents just slightly less than the tunnel values.

The data in Fig. 7 suggest a slight upward response at liquid water contents above 2 g m^{-3}. Since there is no intrinsic physical reason why the probe should behave this way, the most likely explanation lies in the nonlinearity of the tunnel calibration. The calibration curve for 75 m s^{-1} in Fig. 1 shows decreases from linearity at LWC above 2 g m^{-3}. If this decrease was not real, and the response of LWC to nozzle flow rate was closer to linear, some of the slight positive nonlinearity of Fig. 7 would be removed.

b. Selected probes, all conditions

Data from the CSIRO-made probe operated with a wire temperature of 180°C for conditions of $-28 < T_a < 10$°C and $15 < v < 100$ m s^{-1} are shown in Fig. 8. Figure 8 includes all the data for this probe except for a series of three consecutive runs at −15°C which gave

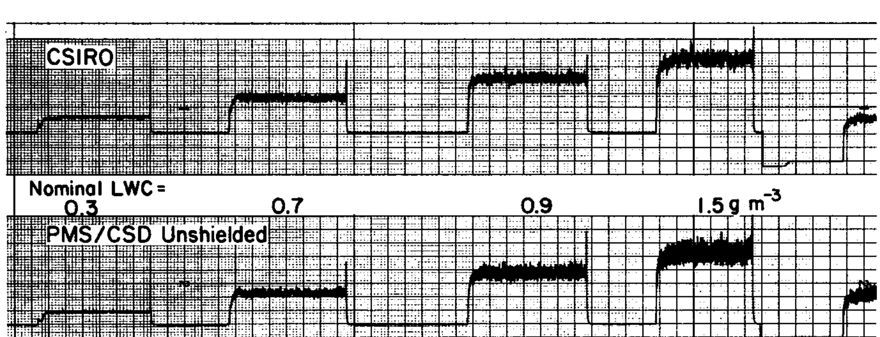

FIG. 6. An example of a chart record showing output voltages run at the indicated LWCs for +10°C and 75 m s^{-1} for the CSIRO-made probe and PMS probe with short sensor. The voltage and time scales are 100 millivolt per division and five seconds per division, respectively. Fine adjustments to the flow rate are made during the first 5–10 s of each LWC setting.

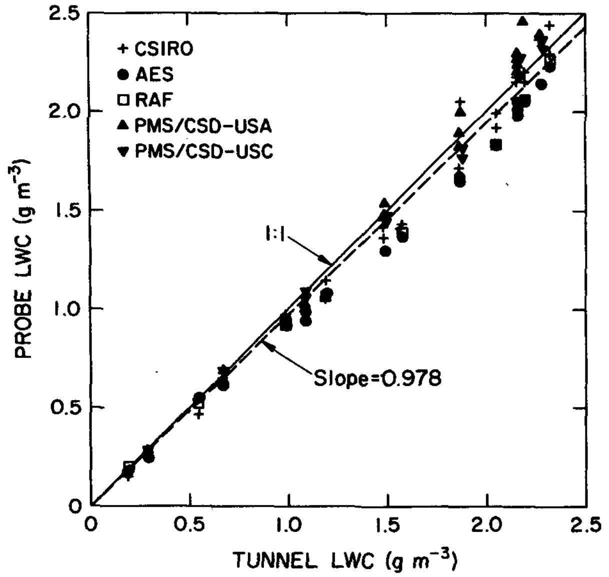

FIG. 7. The LWC measurements from all probes and sensors operating with proper set-up conditions for an air temperature of 10°C and airspeed of 75 m s^{-1} plotted as a function of the LWC derived from the icing cylinder calibration of the tunnel.

consistently less LWC than all other runs. These runs will be discussed separately in Section 6j. Again, the remaining data are quite consistent over the whole range, with a best-fit slope of 0.984.

A comparable data set over a similar range of conditions from two short unshielded probes of diameter 1.76 mm and 2.01 mm is shown in Fig. 9. Again, the scatter is reasonable, with a best-fit slope of 1.002.

It is quite apparent from Figs. 7, 8 and 9 that the differences between the CSIRO-made probes and the *modified* PMS probes are minimal, and the shorter probes ($l \approx 2$ cm) are in no way inferior to the standard-length units ($l \approx 4$ cm).

6. Other tests

a. Effect of varying yaw angle

For some tests, the angle between the axis of the cylinder and the normal to the flow (the yaw angle) was varied from 0 to 20 degrees. Tests were performed on a PMS standard length and short length probe, and the results are shown in Fig. 10. It is apparent that departures from the expected $\cos\theta$ variation due to reduced collection area are minimal up to angles of 20 deg for both probes. Thus, typical aircraft flight conditions in which either angles of pitch or yaw rarely exceed 10 deg, are unlikely to produce errors of any consequence.

b. Effects of varying the operating temperature

Some confusion exists concerning the appropriate operating temperature for the probe. In the first publication on the device, King *et al.* (1978) recommended an operating temperature of about 90°C based on an incorrect supposition that higher temperatures could cause the onset of film boiling and thus slow the evaporation of drops. A later publication (King *et al.*, 1981) showed this was unlikely to occur, and presented reasons why temperatures as high as 160°C could not be considered excessive.

In the tests described here, the wire temperatures of two probes, a PMS/CSD shielded and CSIRO-made unshielded, were varied and the probe response observed. The temperatures referred to in this section are the temperatures calculated from the bridge resistors (see King *et al.*, 1978) and are sufficiently accurate to demonstrate the effect of response to wire temperature. For aircraft usage, when trying to determine the dry term, more precision is required and the nonlinear regression technique is recommended.

Results for the unshielded probe at 75 m s^{-1}, 10°C are shown in Fig. 11a. Even with the usual scatter in the data points, it is apparent that the unshielded probe response increases with temperature for wire temperatures at least as high as 180°C. However, by 247°C the data suggest that the probe response has decreased, in line with the proposition that the film boiling may start to occur at these temperatures.

The results are consistent with laboratory tests conducted at a velocity of about 25 m s^{-1} using a spray device (Dye, 1983) that produces a droplet spectrum with a mean volume diameter of about 15 μm. Results of two series of tests (at nominal LWCs of 0.5 and 1.0 g m^{-3}) in which the wire temperature was varied between 90 and 210°C are shown in Fig. 12. Here the

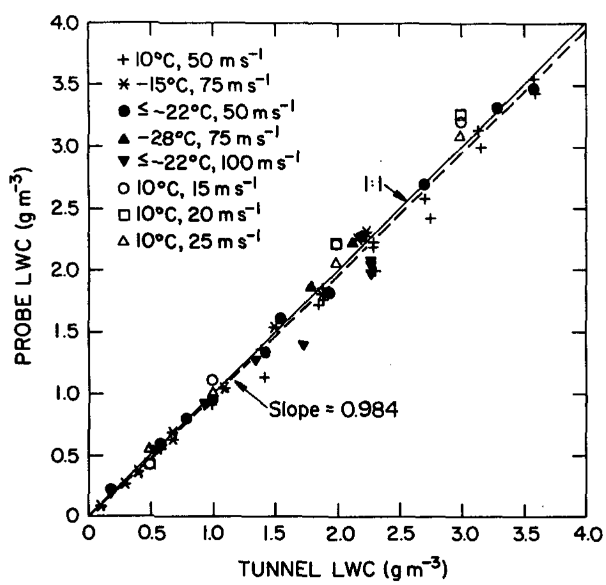

FIG. 8. LWC from the CSIRO-made probe versus the tunnel LWC for the entire range of air temperatures and airspeeds tested.

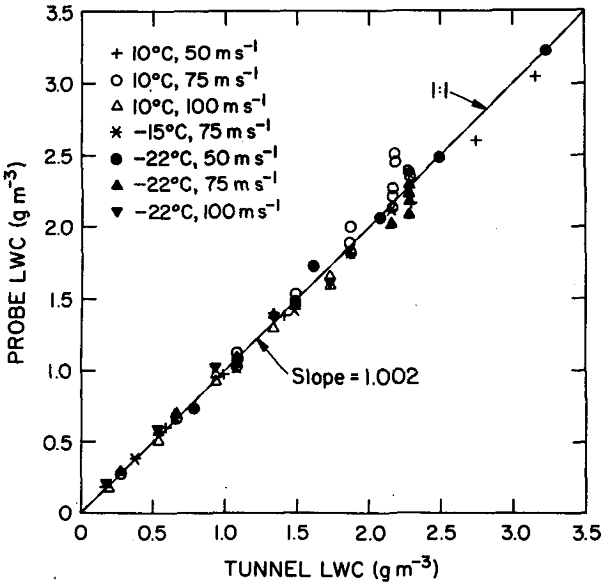

FIG. 9. As in Fig. 8, but for the PMS short probe with unshielded sensors.

increase in output response with increasing wire temperature is smaller than that found in the wind tunnel, but this is to be expected due to the lower velocity and lower heat loading on the wire.

Results for the shielded probe, shown in Fig. 11b, reveal a similar trend. The wire temperature given refers to the calculated temperature of the inner wire. When compared to the unshielded probe, it is apparent that with the present probe construction, the inner wire needs to be run at least 60°C warmer than the unshielded version to obtain the same response. This 60°C differential is due to the gap between the metal shield and the inner wire. Although there is scatter in the data, they do suggest that the temperature difference is greatest when there is a greater heat load on the sensor, as one might expect. Since the optimum temperature of the unshielded probe appears to be around 180–200°C, the shielded one should probably be run at least as high as 240°C. Attempts to do this in the wind tunnel resulted in failure of the sensors, although prolonged operation at 220°C was possible. At this temperature, the response is about 0.9 of that of the unshielded probe, so for those situations in which robustness is of prime concern, the shielded probe offers some advantages with a small, but reproducible decrease in response. It is also expected that improvements in construction techniques such as using fine transformer winding wire with higher temperature coatings and decreasing the gap between the inner wire and outer shield to less than 0.02 mm, would give a longer life at higher temperatures. The shielded sensors used in these tests were among some of the first constructed and tested. Subsequent tests of recently constructed shielded sensors in the PMS wind tunnel, suggest that the response is near that of the unshielded sensors.

c. Effect of airspeed

None of the probes exhibited any airspeed dependent effects. Examples of runs for two probes for speeds between 15 and 100 m s^{-1} have already been shown in Figs. 8 and 9. For this droplet spectrum with an upper limit near 30 μm, there is no evidence of any fall off in response (such as could be caused by splashing) with increasing speed, in line with the previous findings of King *et al.* (1981).

d. Effect of ambient temperature

The only instances of possible temperature related effects occurred for the CSIRO-made probe on a series of three successive runs as noted earlier. No other probes showed any significant differences between its response at 10°C and at temperatures of −15°C or colder. Indeed the responses for all other CSIRO-made probe runs, even at −28°C, were normal. Data from all probes at −15°C or colder is shown in Fig. 13. Tunnel observations also showed that the de-icing on the PMS probe tips was very effective, since no rime buildup was ever observed on a PMS probe tip or element, even at −28°C when the ice buildup on the mounts, etc., was up to 5 cm thick. In this respect, the PMS version of the probe would appear to be superior to the JW probe, since Strapp and Schemenauer (1982) reported that 10 of the 14 JW sensors tested by them at 100 m s^{-1}, −15°C, displayed substantial signal deterioration due to ice buildup, with a more rapid deterioration of performance at colder temperatures.

e. Replacement heads

In all cases, replacement of a probe element with one of a similar type produced little effect on the measured LWC. An example of two successive runs with two different probe heads is shown in Fig. 14. However, it should be noted that in these tests the LWC was determined from a direct measurement of the wet power P_w. Complete interchangeability of probe elements, such that the dry power remains unchanged,

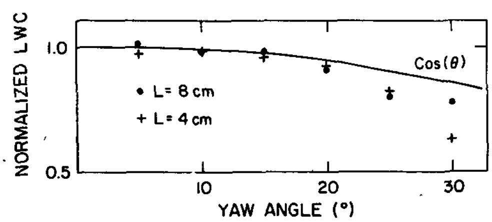

FIG. 10. Sensitivity of the standard (AES) and shorter (PMS unshielded) length probes and sensors to yaw angle.

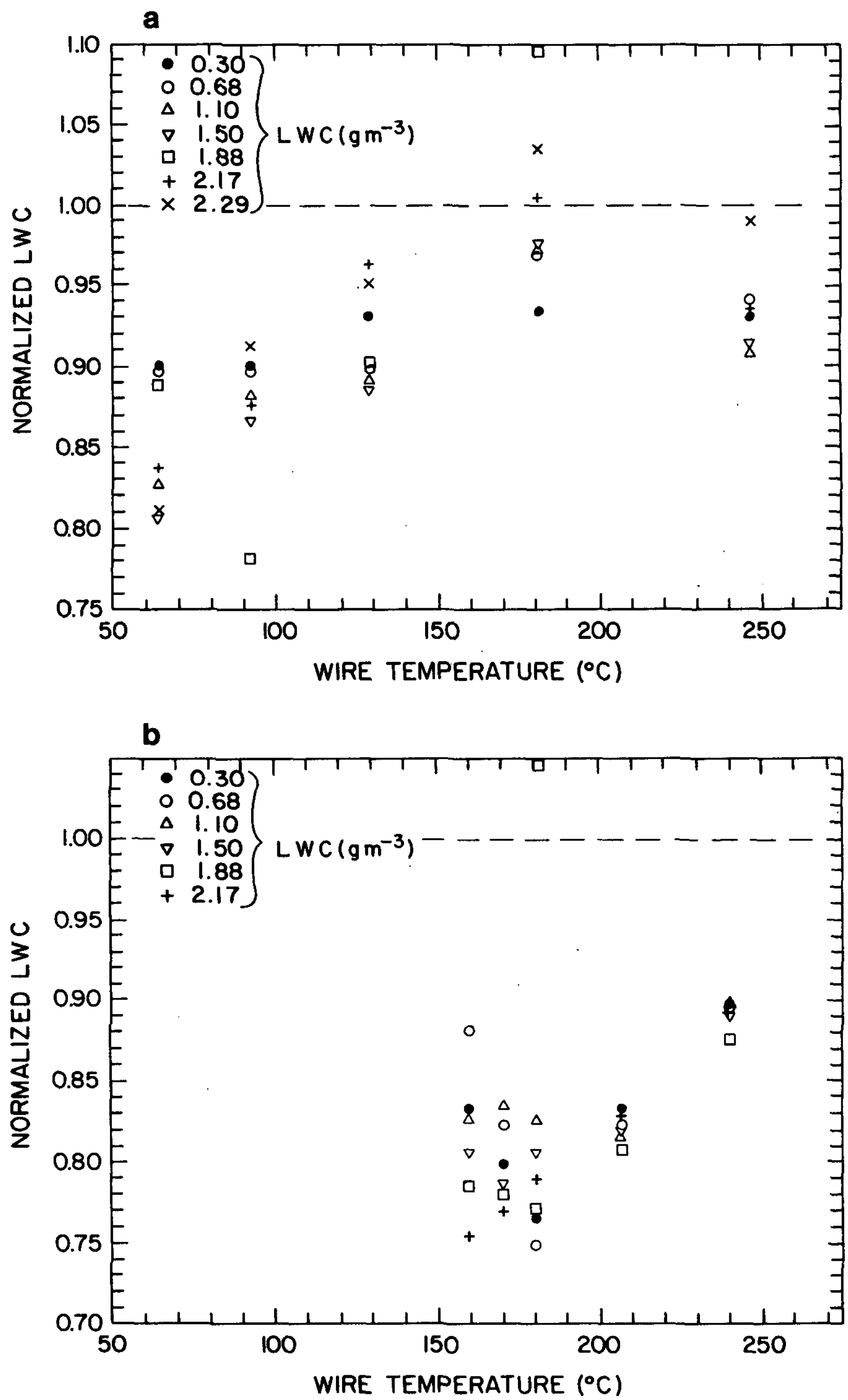

FIG. 11. Sensitivity of the probe output to variation in the wire operating temperature at 10°C and 75 m s^{-1}, (a) the CSIRO-made probe and sensor, and (b) the PMS short probe with shielded sensor. The probe measured LWCs were normalized to the tunnel LWCs shown in the legend.

requires tolerances in all stages of element manufacture that are difficult to achieve. Dimensional tolerances of the order of 1% are comparatively easy to obtain, but winding the wires to a similar resistance tolerance is difficult due to stretching of the fine copper wire. An examination of similar probe elements showed a spread

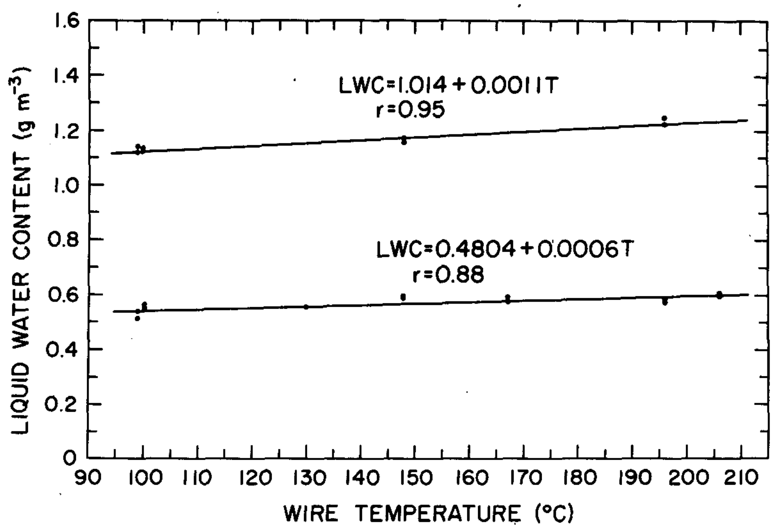

FIG. 12. Sensitivity of the measured LWC from the PMS short probe and unshielded sensor to wire operating temperature from laboratory tests using a spray device at approximately 20°C and approximately 25 m s^{-1}.

of resistance values of 3%. For a fixed bridge ratio, this in turn produces an operating temperature spread of about 6%, necessitating a separate dry calibration for each element. Selection of matched elements after manufacture seems to be the most likely means of achieving complete interchangeability.

f. Effects of power supply voltage

Ignoring considerations of evaporation time, splashing, etc., the value of LWC at which the probe saturates is determined by the availability of power to evaporate the water. This in turn is determined by such parameters as probe dimensions, air velocity, and power supply voltage. Examples of the responses of two probes, a standard length and short version, to decreasing the power supply voltage below 28 V are given in Fig. 15. Conditions were 2.5 g m^{-3} at 75 m s^{-1} at −15°C. It is apparent that the standard length probe performance degrades severely under these conditions when the supply voltage drops much below 26 V, whereas the shorter probe is unaffected for supply voltages as low

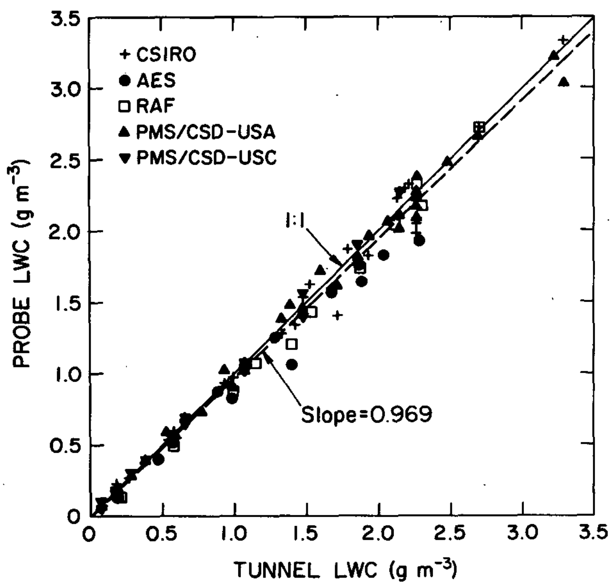

FIG. 13. LWC measured by all probes at air temperatures of −15°C or colder.

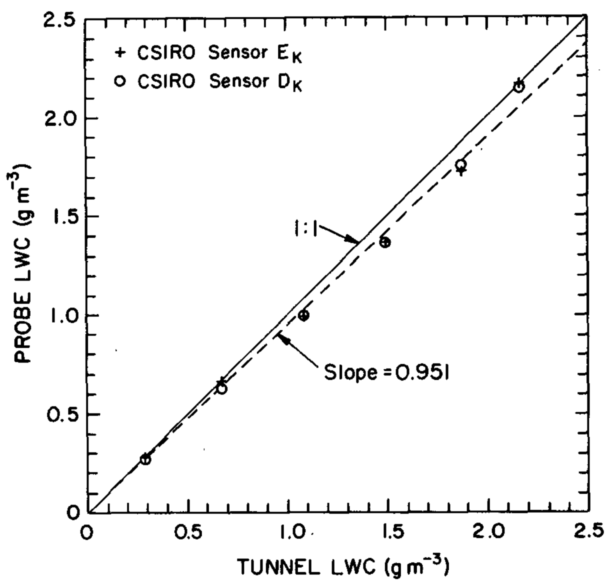

FIG. 14. Results obtained from the CSIRO-made probe with two separate sensors.

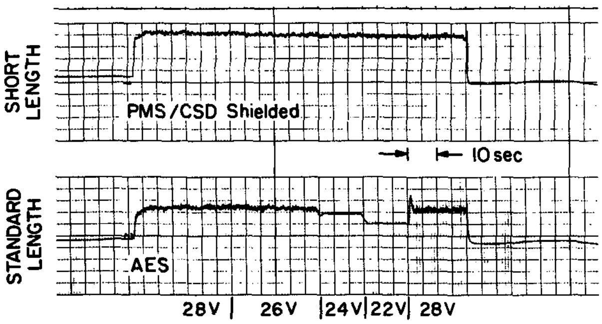

FIG. 15. A chart record showing the response of the PMS short probe with shielded sensor and the PMS standard probe to changes in supply voltage. The drift in the dry power with time was due to the air velocity decreasing as ice built up in the tunnel during the long time of this series of tests.

as 22 V. This feature represents one of the major advantages of the short probe—the voltage required to drive the probe for given conditions is directly proportional to the length and diameter of the element. Thus the shorter probes should be capable of measuring higher LWCs than the longer probes. Additionally, prospects are good for operating a short probe on a 12 V supply, such as in a sailplane or for remote ground use.

g. *Offset voltage and its effect on damping*

For many users of the CSIRO probe, determination of the offset voltage required for correct damping represents the least understood characteristic of the device. In fact, many users are unaware of the potential errors involved in ignoring this aspect. The problem is partly due to the apparent simplicity of the servo-loop which controls the hot-wire temperature, and partly due to the fact that the probe appears to perform quite well without undue attention to the damping characteristics. A detailed treatment of the characteristics of the servo-loop has been given in Bradley and King (1979), but we will derive a much simplified version of it here for the purpose of explaining some of the features from a user's point of view.

Consider the schematic of Fig. 4 with all of the fixed bridge resistors, R_1, R_2, R_3, set to 1 Ω for the sake of simplicity. The important equations governing circuit behavior are as follows:

Amplifier input:

$$V_{\text{in}} = V_+ - V_- = \frac{V_s}{2}\frac{(1 - R_w)}{1 + (R_w)}. \qquad (2)$$

Amplifier transfer equation:

$$\tau \dot{V}_s + V_s = G(V_{\text{in}} + V_{\text{off}}), \qquad (3)$$

where the dc gain is G, V_{off} is the input offset voltage, and the amplifier gain roll-off occurs near a frequency $(2\pi\tau)^{-1}$. Combining (2) and (3), we have

$$\tau \dot{V}_s + V_s = \frac{GV_s}{2}\frac{(1 - R_w)}{(1 + R_w)} + GV_{\text{off}}. \qquad (4)$$

The differential equation describing how the wire resistance varies with time is

$$B\dot{R}_w = \frac{V_s^2 R_w}{(1 + R_w)^2} - P_l, \qquad (5)$$

where B is a constant related to heat capacity, etc., and P_l the rate of heat loss from the wire. The important feature here is not the exact form of (5), but rather that the relationship between R_w and V_s is a rate process, necessitating differentiation of (4) before any substitutions can be made. Then (4) becomes

$$\tau \ddot{V}_s + \dot{V}_s = \frac{G(1 - R_w)\dot{V}_s}{2(1 + R_w)} - \frac{GV_s}{2}\frac{\dot{R}_w}{(1 + R_w)}, \qquad (6)$$

where we have ignored the second-order effect of the rate of change of $(1 + R_w)^{-1}$.

But from (4), we may ignore $\tau \dot{V}_s$ if the fluctuations in V_s occur at frequencies much lower than the cutoff frequency of the amplifier $(2\pi\tau)^{-1}$, giving

$$\frac{G(1 - R_w)}{2(1 + R_w)} \approx 1 - GV_{\text{off}}/V_s. \qquad (7)$$

Substituting back into (4), we then have

$$\tau \ddot{V}_s + \frac{GV_{\text{off}}}{V_s}\dot{V}_s + \frac{GV_s}{2}\frac{\dot{R}_w}{(1 + R_w)} = 0. \qquad (8)$$

Now, provided the second and third terms of (8) can be linearized (and we can always pick a sufficiently small range of R_w and V_s) then (8) can be placed in the form of a second-order linear differential equation which describes a damped oscillator if and only if GV_{off}/V_s remains positive, largely irrespective of the details of how R_w depends on V_s. Indeed, the value of GV_{off}/V_s determines the damping factor in a manner given in Bradley and King (1981) or any standard physics text (e.g., Feynman *et al.*, 1963). The features of importance here are (i) a positive V_{off} is required if the circuit is not to oscillate, and (ii) the required V_{off} is a function of V_s (see Bradley and King for an explanation of why the required V_{off} is actually proportional to V_s^2). Thus a circuit that is sufficiently damped at a low V_s, such as might be found in laboratory testing, may oscillate at higher V_s, such as in aircraft penetrations of cloud. Any signs of excessive noise or oscillations at higher V_s should be used as evidence that more damping is required. As recommended by Bradley and King, an effective method for setting the damping is to impose the maximum expected heat load on the wire, for example by bringing it into contact with a wet tissue, and then adjusting the damping such that it is critically damped for this heat load. (It is prudent to disconnect the slave coils before conducting the test.) It will then be overdamped at lower heat loads, but for aircraft usage not generally by more than a factor of three.

There are a number of ways to alter V_{off} (one of which is via the trim capability of amplifier A_1), but we have found it more convenient to insert a positive voltage to the fixed resistor arm of the bridge. Early CSIRO models and the current PMS model achieved this by having a constant voltage source fed via a variable resistor (see Fig. 4). This works reasonably well for a limited range of V_s, but if V_+ approaches the fixed voltage value V_2, as it can do at high LWC, then in fact there is no current flow and no effective offset. A better way to maintain a constant V_{off} is to feed a constant current source into the bridge arm (again see Fig. 4), and this is the technique currently being used in CSIRO models.

Figure 16 shows the effect of changing the offset and damping on a standard PMS probe. Note the way in which the "noise" is reduced as the offset is increased. This "noise" is the combination of real LWC fluctuations in the tunnel plus electronic oscillation of the probe. The increase in the dry level as the damping is increased is due to a rise in temperature of the wire—the wire resistance increases with offset voltage in accordance with (7). This effect can cause measurement errors at high LWC and high damping levels using the old version of offset voltage, because the offset current actually decreases as V_s increases, and as a result the wire actually runs cooler when water is sprayed on it. The result is a decrease in probe sensitivity under high damping, as can be seen from Fig. 16. On the other hand, if the offset current is kept constant, as in present CSIRO models, there is no decrease in sensitivity until the circuit can no longer supply constant current. This occurs when the voltage at the center of the bridge gets sufficiently high for the collector–emitter voltage on the transistor to fall below the minimum required for it to operate. Under normal conditions, the probe would already have been limited due to insufficient supply voltage (see Section 6f) before this situation arises. Figure 17 illustrates that the CSIRO-made probe maintains uniform sensitivity over a wide range of offset currents. Note that the probe time constant (determined from the probe response to nozzle shut-off) is also affected.

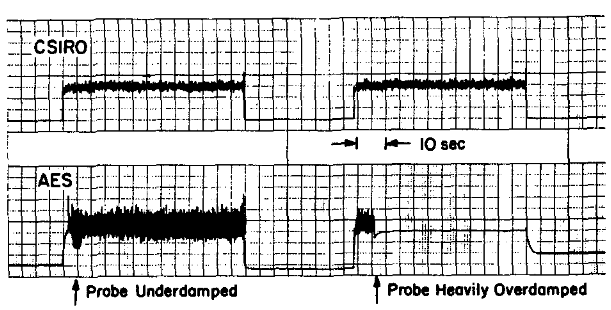

FIG. 16. The effect of offset current on the damping and response of a standard PMS probe. The response from a properly damped CSIRO-made probe is shown above.

Before leaving this section on damping, two further points need to be made. Because the offset voltage of (8) is the sum of the externally introduced voltage and the intrinsic offset of amplifier A_1, replacement of this chip for any reason necessitates rechecking the level of external offset. Second, the effect of the small inductance of the hot-wire elements acts as a stabilizing influence on the circuit, i.e., less offset is required for higher inductances, while the inductance of resistor R_1 has a destabilizing effect (Freymuth, 1977). Thus if resistor R_1 is to be hand-wound, it should be done in a noninductive, i.e., bifilar, manner.

h. Long-term stability

One of the probes and control boxes (RAF) had been tested in the NRC tunnel in a similar fashion six months prior to the tests described here. Modification (i) of Section 3 had not been performed on the probe at that time, so that in performing comparisons with later data, we have made allowance for the lead-wire effects in accordance with the expression given in King *et al.* (1978). This amounted to a 3% decrease in the measured response. Comparison data for this probe operated at the same temperature of about 140°C, for the earlier and present tests, is shown in Fig. 18. The difference between the two curves is within the experimental error, indicating that the probe response to liquid water is stable over long time periods.

i. Inoperative slave wires

In two of the tests, the slave wires were completely disconnected. For the standard length wire, this caused an apparent increase in measured LWC of only 5% at 2.0 g m^{-3}, 75 m s^{-1}, +10°C. For the short, unshielded, 2 mm diameter probe, the increases ranged from 9% at 0.7 g m^{-3} to 25% at LWC in excess of 1.8 g m^{-3} (all at 75 m s^{-1}, 10°C). The effect on the standard length probe was less than anticipated, and indicates that for this probe, loss of the slave wires would not produce catastrophic measurement errors. However, for both probes, but particularly the shorter one, we strongly recommend monitoring the operation of the slave windings, since inspection of the data will not in general be sufficient to detect a problem. This is most easily performed by measuring the voltage across the fixed resistor in series with the slaves and putting it in a form suitable for use as a status bit on data acquisition systems.

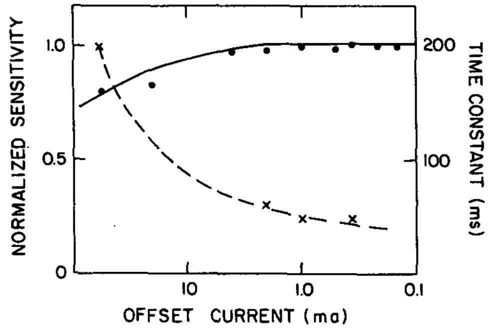

FIG. 17. The normalized response (dots) and time constant (×) of the CSIRO-made probe as a function of the resistance used to control the offset current.

j. Inconsistencies

In Section 5b, we mentioned three consecutive runs in which the CSIRO probe produced values which were about 10% lower than any of the other 47 runs made with the probe. For these runs, the other probe in the tunnel did not display similar decreases. Apparently there was an unexplained temporary fault in the probe. There were also other isolated instances of anomalous results. For example, the results for both probes in the tunnel for run 74 were about 10% lower than the mean response from other runs for these probes but within 3% of each other—an indication that, in this case, the tunnel values were low. Stallabrass (1978), in his discussion of calibration of the tunnel, mentions a similar odd result for which there was no obvious explanation and several of the present authors have observed similar occurrences in previous tests. The point we wish to make here is that the types of comparisons described in this paper are of one instrument against another, not a calibration of one against an absolute. We would agree with Stallabrass that the icing cylinder technique is the most fundamental standard available for comparisons, but an icing wind tunnel is an extremely complex electrical and mechanical facility and it is impractical to continuously monitor its performance using icing cylinder techniques. Thus, even in a well-maintained facility such as the NRC tunnel, it should not be unexpected that a few anomalous data points defying easy explanation will occur.

7. Conclusions

The results demonstrate that the CSIRO probe represents an advance in instrumentation for the airborne measurement of LWC. The icing wind tunnel tests have shown that correctly operated probes will measure to better than within 15% of values calculated using the icing cylinder technique, the most fundamental means that we presently have for the measurement of LWC. Differences in response for all properly operating units were rarely more than 10% and always less than 15%, except for the shielded ones. Because the response of the probe to LWC can be calculated directly, the need for a separate wet calibration is eliminated.

The current standard length probe may be subject to damage in heavy graupel or hail, but smaller versions, particularly the shielded ones, represent an improvement in this regard.

Similar tests by Strapp and Schemenauer (1982) conducted in the same facility for the JW probe showed significant occurrences of air speed dependence, unpredictable calibration changes with change of sensor head, and increasingly severe icing problems at temperatures less than −15°C. For LWCs less than 1.9 g m^{-3} at −5°C, at most 75% of the probes tested by Strapp and Schemenauer agreed to within 20% of tunnel LWC values. By comparison, in the present study all but a few percent of all points from all tests and probes (including improperly operated and shielded probes) were within 20% of the tunnel values. From these observations, it appears that the performance of the CSIRO designed system is superior to that of the JW in many key aspects of cloud droplet LWC measurements. It has not had the same extensive operational field testing as the JW probe, and more flying hours are required before a realistic assessment of its field usage can be made. Also, it should be noted that unlike the JW probe, which has a cutoff in response for droplets larger than 40 μm diameter, laboratory and field tests have shown the CSIRO probe to have partial response to drizzle and precipitation-size drops.

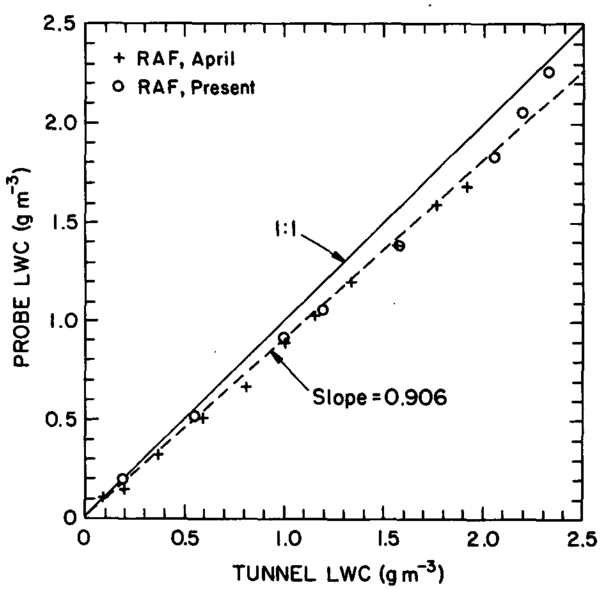

FIG. 18. Results obtained from tests of a PMS standard probe in the NRC icing tunnel in April and again in October of 1983, illustrating the long-term stability of the response.

Specific conclusions that can be drawn as the result of tests described in this paper include:

i) The commercial PMS version, modified as noted earlier, does not behave differently from the CSIRO version except in two areas: the insertion of the offset current (which detracts from performance) and de-icing of probe tips (which is superior to the CSIRO version).

ii) The performance of the short probes is comparable with that of the standard length units. Variations in diameter of 50% also produced no measurable differences in performance.

iii) The operating temperature for unshielded versions should be of the order of 180°C. For shielded versions, it should be at least 220—240°C if construction will allow—and improved construction techniques are needed to accomplish this.

iv) Setting the correct offset voltage is important—an overdamped probe will result in a decreased response.

v) For the standard 8 cm length probe at 2 g m^{-3} at 75 m s^{-1}, probe performance will degrade if the supply voltage is less than 26 V. For higher LWC and speeds, it is recommended that a shorter length probe be used.

vi) Corrections for yaw angles less than 15 deg are less than 3% for both probes lengths, and hence can be ignored.

vii) Operation without the slave windings produces errors of the order of 5% for 2 g m^{-3} in a standard length probe, but up to 25% in the shorter probe. Separate recording of the slave wire status is strongly recommended.

For airspeeds of 100 m s^{-1} these tests were conducted with LWCs less than 2 g m^{-3} using drop size spectra with median volume diameters of 20 μm and cutoffs less than 40 μm. Separate quantitative studies to examine the probe response to higher LWC (e.g., 4 to 5 g m^{-3}) at typical aircraft speeds and to drizzle and precipitation-size drops are needed.

Acknowledgments. The authors wish to acknowledge the technical assistance of D. Turvey (CSIRO), W. Grotewold (NCAR), and M. Wasey (AES). M. Parker and R. Gibson of CSIRO were responsible for the improvement in offset voltage insertion. C. Biter and B. Ruiz helped in some aspects of data reduction. The authors are also grateful to Mr. T. R. Ringer of the Low Temperature Section of the Mechanical Engineering Division of the National Research Council of Canada for the use of their excellent facility and to R. Price for operating the tunnel and assisting with the tests.

REFERENCES

Baumgardner, D., 1983: An analysis and comparison of five water droplet measuring instruments. *J. Climate Appl. Meteor.*, **22**, 891–910.

Bradley, S. G., and W. D. King, 1979: Frequency response of the CSIRO liquid water probe. *J. Appl. Meteor.*, **18**, 361–366.

Dye, J. E., 1983: A spray device for ground testing of the Johnson–Williams liquid water content meter. *Preprints, Fifth Symp. Meteorological Observations and Instrumentation*, Toronto, Amer. Meteor. Soc., 362–371.

Feynman, R. P., R. B. Leighton and M. Sands, 1963: *Lectures in Physics, Vol. I.* Addison Wesley, 468 pp.

Freymuth, R., 1977: Frequency response and electronic testing for constant-temperature hot wire anemometers. *J. Phys. E: Sci. Instrum.*, **10**, 705–710.

King, W. D., D. A. Parkin and R. J. Handsworth, 1978: A hot-wire water device having fully calculable response characteristics. *J. Appl. Meteor.*, **17**, 1809–1813.

——, C. T. Maher and G. A. Hepburn, 1981: Further performance tests on the CSIRO liquid water probe. *J. Appl. Meteor.*, **20**, 195–202.

Langmuir, I., and K. B. Blodgett, 1961: A mathematical investigation of water droplet trajectories. *Collected Works of Irving Langmuir*, Pergamon, **10**, 348–393.

Lozowski, E. P., J. R. Stallabrass and P. F. Hearty, 1983: The icing of an unheated, nonrotating cylinder. Part II: Icing wind tunnel experiments. *J. Climate Appl. Meteor.*, **22**, 2063–2074.

Stallabrass, J., 1978: An appraisal of the single rotating cylinder method of liquid water content measurement. Tech. Note LTR-LT-92, National Research Council, Canada, 40 pp.

Strapp, J. W., and R. S. Schemenauer, 1982: Calibrations of Johnson–Williams liquid water content meters in a high-speed icing tunnel. *J. Appl. Meteor.*, **21**, 98–108.